J Comput Electron (2013) 12:388–396
DOI 10.1007/s10825-013-0480-9

Decoherence effects in the Wigner function formalism

Philipp Schwaha · Damien Querlioz · Philippe Dollfus · Jérôme Saint-Martin · Mihail Nedjalkov · Siegfried Selberherr

Published online: 12 June 2013

Abstract We demonstrate the ability of the phase space formulation of quantum mechanics to provide convenient means and intuitive notions for exploring the process of transition from a quantum to a classical state known as decoherence. The Wigner equation, which is usually relevant for electron transport in nanostructures, augmented by the Boltzmann scattering operator is now applied to the time dependent transport problems which may be considered as benchmark examples for the decoherence role of phonons in semiconductor devices. Simulation results maintained by theoretical analysis show how scattering effectively destroys the interference effects. The initial coherence in the wave vector distribution is pushed towards the equilibrium distribution. In particular scattering by phonons hinders the natural spread of the density with time and advances it towards a classical localization. Furthermore, the decoherence effect due to phonons, is measured by the purity of the Wigner state, which decreases from its initial value of 1, with a rate depending on the lattice temperature, and by a functional comparing diagonal with off-diagonal elements of the density matrix.

Keywords Wigner function · Quantum transport · Phonons · Decoherence

P. Schwaha · M. Nedjalkov (✉) · S. Selberherr
Institute for Microelectronics, TU Wien, 1040 Wien, Austria
e-mail: nedjalkov@iue.tuwien.ac.at

P. Schwaha
e-mail: philipp@schwaha.net

S. Selberherr
e-mail: selberherr@iue.tuwien.ac.at

Present address:
P. Schwaha
AVL List GmbH, Hans-List-Platz 1, 8020 Graz, Austria

D. Querlioz · P. Dollfus · J. Saint-Martin
Institut d'Electronique Fondamentale, Université Paris-Sud, CNRS, 91405 Orsay, France

D. Querlioz
e-mail: damien.querlioz@u-psud.fr

P. Dollfus
e-mail: philippe.dollfus@u-psud.fr

J. Saint-Martin
e-mail: jerome.saint-martin@u-psud.fr

1 Introduction

The theory of decoherence addresses the manner in which some quantum systems become classical due to entanglement with the environment. The latter monitors certain observables in the system, destroying coherence between the states corresponding to their eigenvalues. Only preferred states survive consecutive interactions with the environment. The remainder of states, which actually comprises a major part of the Hilbert space, is eliminated. Many of the features of classicality are actually induced in quantum systems by their environment [1]. The Wigner function has often been used in atomic physics to study decoherence [2, 3], because it makes the transition towards the semi-classical world very clear by tending to a distribution function. Additionally, it has been recently demonstrated that the superposing photon states prepared in an electromagnetic resonator can be completely characterized by Wigner's function tomography [4].

Regarding solid-state nanodevices, decoherence in the transport through quantum dots coupled to quantum point contacts has been discussed within the concept of pointer states [5]. Alternatively, a theoretical description of decoherence induced by contact coupling in ballistic nanodevices

has been established within the framework of open system theory [6].

The role of scattering has been intensively studied by different models describing quantum Brownian motion [7]. Peculiar to the equation governing the evolution of the density matrix in the spatial coordinate representation $\langle x|\hat{\rho}|x'\rangle$ is a term giving rise to an exponential damping in time with a rate Λ of the off-diagonal elements ($x \neq x'$). Thus the initial wave packet of an electron does not follow the natural process of spreading due to coherent evolution, but shrinks around the line $x = x'$ revealing a classical localization [7].

The electron decoherence induced by electron-phonon interaction has been considered in a molecular conductor in the language of Landauer's approach of transport by means of Green's function calculation [8]. This decoherence effect on an electron has also been investigated in a bulk semiconductor by evaluating the time evolution of the generalized Wigner function of the electron-phonon system for a single electron/phonon scattering event by using the "Wigner paths" method [9].

Recently the problem has been reformulated in phase space giving rise to a Wigner equation with a Fokker-Planck term describing diffusion in phase space [10]. The analysis of the equation provides an alternative interpretation of the process of decoherence in phase space. Quantum coherence effects as a rule give rise to rapid oscillations of the Wigner function. The diffusion term destroys these oscillations thus effectively suppressing coherence. Furthermore, this model has been compared with the Wigner-Boltzmann equation showing that both models converge provided that the wave vector of the lattice vibrations in the latter model becomes much smaller than the electron counterpart [10]. It follows that decoherence effects can definitely be expected as a result of scattering by phonons. Theoretical analysis shows that an increase of the electron-phonon coupling leads to a super-linear decrease of the quantum contribution [11] due to a decrease of the proportion of the coherent component of the Wigner-Boltzmann equation and an interplay between the scales of the involved physical parameters, formally expressed as the limit $\hbar \to 0$.

The effects of decoherence will be demonstrated by Monte Carlo simulations of the evolution of a single wave packet tunneling trough a potential barrier, and of a pure Wigner state consisting of two entangled Gaussian wave functions.

The paper is organized to first provide an outline of the theoretical foundations. It starts, in Sect. 2.1, by describing the physicals principles and ideas involving the Wigner formulation of quantum mechanics and the connection to the density matrix formalism. Section 2.2 introduces the Wigner-Boltzmann equation and its link to classical Boltzmann transport. We then continue, in Sect. 2.3, to describe the Monte Carlo methodologies used in the subsequent calculations.

Simulation results of two distinct approaches using the described theoretical background are given in Sect. 3. In particular Sect. 3.1 deals with a tunneling process simulated using an affinity based approach; Sect. 3.2 studies the decoherence of two entangled states using a generation-annihilation procedure.

2 Quantum mechanics in phase space

We introduce the basic concepts and notions of the phase space formulation of quantum mechanics, which allows to conveniently trace the transition from a quantum coherent to a classical state during the process of decoherence. We continue by recalling the properties of pure and mixed states.

2.1 Density matrix of entangled and mixed states

Consider the basis $|0\rangle|1\rangle$. Any normalized superposition

$$|\psi\rangle = \alpha|0\rangle + \beta|1\rangle \tag{1}$$

gives an entangled state. The expectation values $\langle A\rangle$ of physical quantities A, presented by a Hermitian operator $\hat{A}$, are obtained by the trace operation:

$$\langle A\rangle = \mathrm{Tr}(\hat{A}\hat{\rho}) = \sum_{i=0,1} \langle i|\hat{A}\hat{\rho}|i\rangle; \quad \mathrm{Tr}(\hat{\rho}) = 1. \tag{2}$$

The density operator $\hat{\rho}$ is defined with the help of (1):

$$\begin{aligned}\hat{\rho} &= |\psi\rangle\langle\psi| \\ &= |\alpha|^2|0\rangle\langle 0| + |\beta|^2|1\rangle\langle 1| + \alpha\beta^*|0\rangle\langle 1| + \alpha^*\beta|1\rangle\langle 0|\end{aligned} \tag{3}$$

The physical quantity 'expectation value for the first basis state' in (1), for example, expressed by the operator $\hat{\rho}_0 = |0\rangle\langle 0|$, evaluates to $|\alpha|^2$ using the trace operation, while for the second state it yields $|\beta|^2$. The relation $|\alpha|^2 + |\beta|^2 = 1$ allows to interpret these values as probabilities, which implies the normalization of (1) and ensures the last equality in (2).

In order to ascertain and define quantities we need to prepare a detector which discriminates states $|0\rangle$ from state $|1\rangle$ by virtue of their orthogonality. There are two peculiarities of this process. Such an interaction disturbs the superposition state (1) by leaving it in a preferred state. The probability of finding the system in the alternative state after such an interaction is zero. Moreover, the last two terms in (3) remain unobservable for such a detector. However, they can be observed by an other kind of detector and actually reveal the quantum character of (1): they account for the superposition of the amplitudes which lead to interference effects.

If these interference effects are neglected, the density operator $\hat{\rho}$ reduces to $\hat{\rho}_m = |\alpha|^2\hat{\rho}_0 + |\beta|^2\hat{\rho}_1$. This density operator again provides the values $|\alpha|^2$ and $|\beta|^2$ for the basis

states, however, it corresponds to an entirely different set-up of the system. The latter is in *either* the state 0 with a probability $|\alpha|^2$, *or* the complementary state with the complementary probability which comprises the mixed state density operator $\hat{\rho}_m$. The transition of (1) into one of the two possible basis states as a result of a interaction with the environment gives rise to the same $\hat{\rho}_m$, which is a return to the principles of the classical superposition of probabilities.

2.2 Wigner-Boltzmann equation

For a statistical ensemble of particles described by a density operator $\hat{\rho}$ the Wigner function (WF) f_w is defined in the full phase-space $\mathbf{r}, \mathbf{k}$ as a differential Fourier transform of the density matrix $\rho(\mathbf{r}, \mathbf{k})$, i.e.:

$$f_w(\mathbf{r}, \mathbf{k}) = \frac{1}{(2\pi)^d} \int d\mathbf{r}' e^{-i\mathbf{k}\mathbf{r}'} \rho\big(\mathbf{r} + \mathbf{r}'/2, \mathbf{r} - \mathbf{r}'/2\big) \tag{4}$$

d is the real-space dimension of the transport problem. The dynamical equation of the WF in a potential $U(\mathbf{r})$ is the Wigner transport equation (WTE) which reads:

$$\frac{\partial f_w}{\partial t} + \mathbf{v}\nabla_{\mathbf{r}} f_w = \hat{Q} f_w + \hat{C} f_w \tag{5}$$

$\hat{C}$ is the collision operator and $\hat{Q} f_w$ is the quantum evolution term resulting from the non- local effect of the potential, defined by:

$$\hat{Q} f_w(\mathbf{r}, \mathbf{k}) = \int \mathrm{d}\mathbf{k}' V_w\big(\mathbf{r}, \mathbf{k} - \mathbf{k}'\big) f_w\big(\mathbf{r}, \mathbf{k}'\big) \tag{6}$$

from the Wigner potential V_w given by:

$$V_w(\mathbf{r}, \mathbf{k}) = \frac{1}{i\hbar(2\pi)^d} \int d\mathbf{r}' e^{-i\mathbf{k}\mathbf{r}'} \times \big[U\big(\mathbf{r} + \mathbf{r}'/2\big) - U\big(\mathbf{r} - \mathbf{r}'/2\big)\big] \tag{7}$$

An alternative form for the quantum term $\hat{Q} f_w$ leads to an expansion in powers of $\hbar$ and higher order derivatives of the potential energy [12]. For slowly varying potential the first order approximation of this form reduces to

$$\hat{Q} f_w(\mathbf{r}, \mathbf{k}) = -\frac{1}{\hbar} \nabla_{\mathbf{r}} U(\mathbf{r}) f_w(\mathbf{r}, \mathbf{k}) \tag{8}$$

which is exactly the effect of the classical force on the Maxwell-Boltzmann distribution function in the Boltzmann transport equation (BTE). Thus, the BTE can be seen as the classical approximation of the WTE, if the same collision operator $\hat{C}$ is used in both cases, i.e., if quantum collision effects are neglected. Then, it has been shown that, under a few reasonable conditions, the Boltzmann collision operator can be also used with good accuracy in the WTE [13]. This new form of the WTE is often called Wigner-Boltzmann transport equation (WBTE). It is a strong result and one of the main advantages of the Wigner function with regard to device modelling. All the knowledge acquired in the past in the treatment of scattering in semiclassical transport may be reused for quantum transport in the Wigner formalism. It enables to study important problems such as the scattering-induced decoherence and the transition from quantum to semiclassical transport regimes. Indeed, by Fourier transform of the WF it is straightforward to return to the density matrix and to get direct information on the coherence/decoherence of the system.

In particular, for a single-dimensional transport problem along x-direction and a non-degenerate electron gas, the WBTE reads:

$$\left(\frac{\partial}{\partial t} + \frac{\hbar k_x}{m}\frac{\partial}{\partial x}\right) f_w(x, \mathbf{k}, t) = \int dk_x' V_w\big(x, k_x' - k_x\big) f_w\big(x, k_x', \mathbf{k}_{yz}, t\big) + \int d\mathbf{k}' f_w\big(x, \mathbf{k}', t\big) S\big(\mathbf{k}', \mathbf{k}\big) - f_w(x, \mathbf{k}, t)\lambda(\mathbf{k}) \tag{9}$$

Here, the phase space is formed by a single position and three wave vector coordinates. Quantum correlations are described by the arguments x and k_x of the Wigner potential V_w. Phase-breaking processes are accounted for by the Boltzmann scattering operator with $S(\mathbf{k}, \mathbf{k}')$, the scattering rate for a transition from $\mathbf{k}$ to $\mathbf{k}'$. The term $\lambda(\mathbf{k}) = \int d\mathbf{k}' S(\mathbf{k}, \mathbf{k}')$ is the total out-scattering rate. The Wigner function f_W is a real quantity. Physical averages are obtained according to $\langle A \rangle = \int d\mathbf{k} dx A(x, \mathbf{k}) f_w$, where A is a generic dynamical function in phase space. Thus, f_w resembles the classical distribution function. However, in contrast to the latter, it allows negative values. Actually, the only positive Wigner function is the equilibrium Maxwell-Boltzmann distribution f_{MB}, which is exactly the classical limit of the Wigner function. Moreover, this is the only function which equates the two terms in the scattering operator and thus remains unchanged by scattering.

2.3 Monte Carlo solution of the WBTE

To develop a particle approach for solving the Wigner transport equation, one possibility consists in considering the Wigner function f_w as a sum of Dirac excitations

$$f_i(x, \mathbf{k}, t) = A_i(t)\delta\big(x - x_i(t)\big)\delta\big(\mathbf{k} - \mathbf{k}_i(t)\big) \tag{10}$$

localized in both real and reciprocal spaces. Such excitations or pseudo-particles have a real-space coordinate x_i, a wave vector k_i, and a magnitude A_i which is called affinity, as initially suggested in [14]. This latter parameter is not necessary in semiclassical transport, because the Boltzmann distribution function is always positive, but it is required in order to reconstruct the Wigner function which can locally

assume negative values. It contains the information on the quantum state of the system.

Consistent with the Heisenberg inequalities, such excitations, which we will call pseudo-particles, do not represent physical particles. They are mathematical quantities for the solution of the WBTE. The advantage of this formulation is that the evolution of these excitations follows simple equations [15]. In our "affinity" approach the quantum term $\hat{Q} f_w$ induces the continuous evolution of the pseudo-particle affinity. Pseudo-particles behave and scatter as classical particles, except that the potential does no longer influence the wave vector but only the affinity through the quantum evolution term. The wave vector can change only after a scattering event. The initial method has been improved and extended to study a wide range of nanodevices [16].

Alternatively, the quantum evolution term $\hat{Q} f_w$ of the WBTE can be seen as a scattering term [17], and it can be formally treated this way by introducing an additional "quantum scattering" rate into the Monte Carlo scattering process. When selected, this quantum scattering generates pseudo-particles of positive and negative sign. Since this process may lead to an exponential growth of the particle number, an algorithm making use of annihilation of particles with positive and negative sign has been proposed to obtain convergence. Self-consistence with Poisson's equation has been reported using this technique [18]. In simple cases of uniform potential problems, both "affinity" and "sign" methods are fully equivalent. In the case of the tunnelling problem analyzed below, the "affinity" method has been used, while the evolution of the entangled state has been explored with the particle sign method.

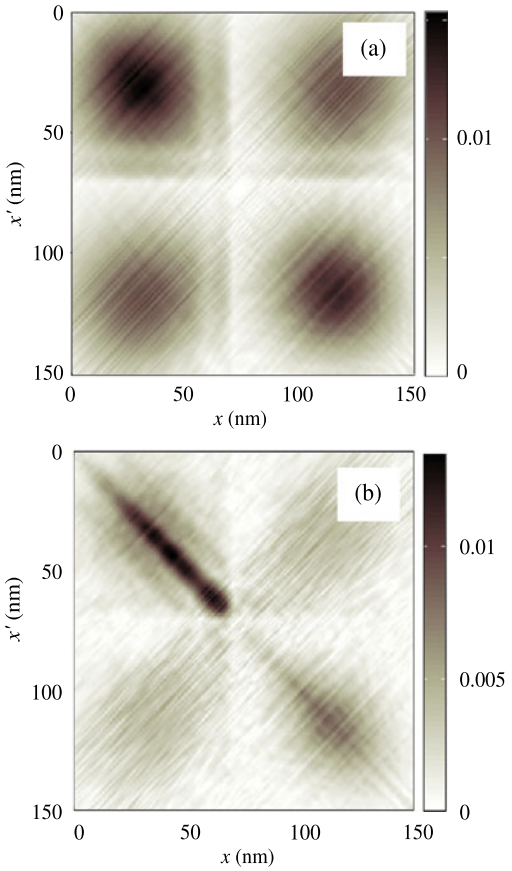

Fig. 1 Modulus of the density matrix of a wave packet after interaction with a tunnel barrier (**a**) without and (**b**) with coupling to a phonon bath. The density matrix elements are expressed in nm^{-1}

3 Simulations

3.1 Tunneling process

The single-barrier structure is a priori likely to generate spatial quantum coherence. If a wave-packet is sent ballistically (with no coupling to the phonon bath) onto a barrier, the resulting reflected and transmitted wave-packets are fully coherent with each other (this is the situation of Fig. 1).

They are parts of the same wave function and, in other words, the electron is fully delocalized over both sides of the barrier: the electron is on the two sides of the barrier at the same time, in a sort of "Schrödinger's cat" state. This situation is well observed in Fig. 1 which shows the density matrix in the case where a ballistic Gaussian wave packet has interacted with a tunnel barrier. The Wigner function of the initial wave packet can be written as:

$$f_w(x,k_x) = N e^{-\frac{(x-x_0)^2}{\sigma^2}} e^{-(k_x-k_0)^2\sigma^2} \tag{11}$$

where N is a normalization constant. The initial transverse momentum of particles is randomly selected according to a thermal law. In the case of Fig. 1, we have chosen $k_0 = 4 \times 10^8\ \mathrm{m}^{-1}$, $x_0 = 30$ nm, and $\sigma = 10$ nm. The barrier is centered at the position $x_C = 75$ nm, its width and height are 2 nm and 0.3 eV, respectively. The picture is taken after 130 fs. The electrons on the left and right sides of the barrier are fully coherent, so high off diagonal values appear in the density matrix, connecting both sides of the barrier. When including phonon scattering the coherence between the left and the right sides of the barrier appears strongly damped. Electrons are separately localized and if interferences between electrons on the left and right sides could be constructed, they would have low contrast.

The Wigner picture provides an insight into the reasons of the classical localization effects. The wave packet is subjected to Fourier transform, hence revealing its spectral momentum composition. The interaction with phonons then acts on each of the components in a randomizing manner, which eventually also destroys all quantum information. The localization can now be explained by the fact that interaction with the phonon environment becomes more likely, thus the

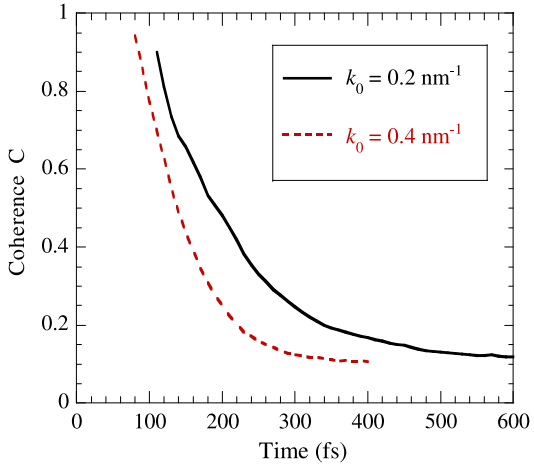

Fig. 2 Coherence C (defined in (12)) between both sides of the tunnel barrier as a function of time after interaction of a wave packet with the barrier, for two initial average wave vectors k_0

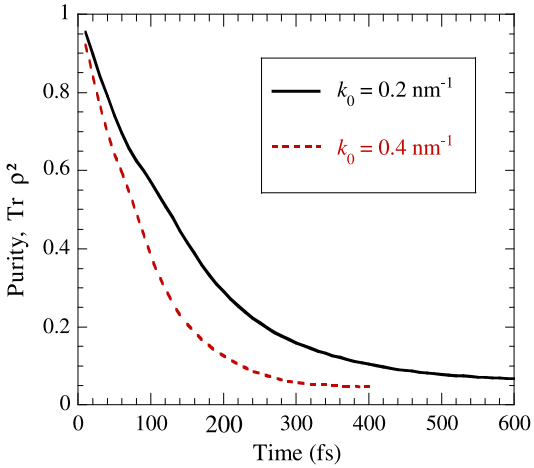

Fig. 3 Purity P (defined in 13) between both sides of the tunnel barrier as a function of time after interaction of a wave packet with the barrier, for two initial average wave vectors k_0

randomizing scattering effects more pronounced, as energy increases. Therefore, the fastest components of a wave packets are affected the strongest leading to localization due to classical scattering effects.

To quantify the localization of electrons on one or the other side of the barrier due to decoherence, we define a "coherence" between the left (L) and the right (R) side of the barrier by:

$$C = \frac{\int_L dx \int_R dx' |\rho(x,x')|}{\int_L dx \sqrt{\rho(x,x)} \int_R dx' \sqrt{\rho(x,x)}} \tag{12}$$

This parameter compares the off-diagonal elements of the density matrix connecting the left and right sides of the barrier to the diagonal elements associated with left and right sides. It is thus equal to unity in purely coherent conditions. It is plotted as a function of time in Fig. 2 for two values of the initial wave vector k_0. It appears that coherence decreases rapidly. An electron, which tunnels through a barrier can rapidly be considered as being on one side of the barrier, but not in a coherent state between the two sides. In more descriptive language, the "Schrödinger's cat" state is quickly resolved by the environment. This justifies the "semiclassical" modeling of tunneling, which simplifies this quantum effect in a transmission probability deduced from the Schrödinger equation. This behaviour may also be quantified by the purity of the density matrix, as commonly used in studies of decoherence.

The purity is defined as $P = \mathrm{Tr}\,\rho^2$. It is a measure of the statistic uncertainty associated with the delocalization of the wave functions. It can be easily shown that the purity may be also defined as [19]:

$$P = 2\pi \int dx \int dk f_w^2(x,k) \tag{13}$$

In the case where phonon scattering is included, the time evolution of the purity is displayed in Fig. 3. A rapid decrease from the initial value of one is observed at short times. It tends to zero with a rate depending on the initial wave vector k_0.

3.2 Decoherence of entangled state

The chosen initial condition is the superposition (1) of two Gaussian wave packages: $e^{-(x\pm a)^2/2\sigma^2} e^{ibx}$ The corresponding initial Wigner function

$$\begin{aligned} f_w^0(x,k_x) = {} & N e^{-(k_x-b)^2\sigma^2} \\ & \times \left(\mathrm{e}^{-\frac{(x-a)^2}{\sigma^2}} + \mathrm{e}^{-\frac{(x+a)^2}{\sigma^2}}\right. \\ & \left. + \mathrm{e}^{-\frac{x^2}{\sigma^2}} \cos\big((k_x-b)2a\big)\right) \end{aligned} \tag{14}$$

comprised by two Wigner wave packets and an oscillatory term is shown in Fig. 4. Equilibrium is assumed in the other two directions of the wave space, so that

$$f_w^0(x,\mathbf{k}) = \frac{\hbar^2}{2\pi mkT} e^{-\frac{\hbar^2(k_y'^2+k_z'^2)}{2mkT}} f_w^0(x,k_x). \tag{15}$$

A GaAs semiconductor with a single Γ valley and scattering mechanisms given by elastic acoustic phonons and inelastic polar optical phonons is considered, while setting the parameter $a = 70$ nm. The choice of

$$2\sigma^2 = \hbar^2/(2mkT) \tag{16}$$

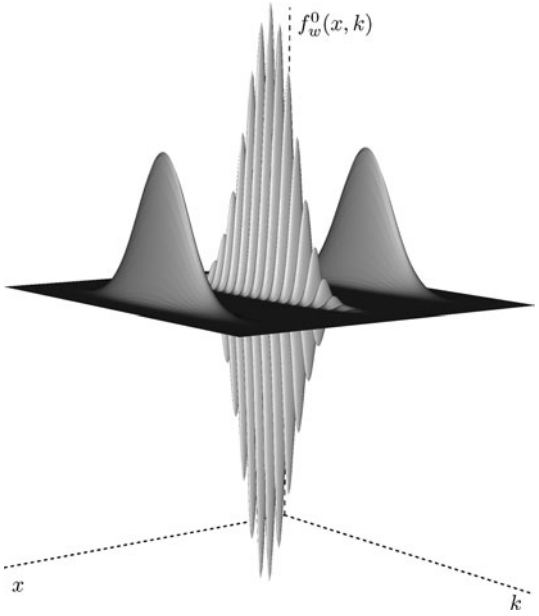

Fig. 4 Entangled wave packets used as initial condition. The two Gaussian functions of the phase space coordinates are separated by a positive and negative values: the oscillations along k_x are in accordance with the last term in (14)

along with $b = 0$ gives rise to $f_{\mathrm{MB}}(\mathbf{k})$, which minimizes the effect of the phonons on the change in the shape of the wave vector distribution. The reversible coherent evolution is characterized by oscillations and negative values of the Wigner function, which are manifestations of quantum superpositions. During a coherent evolution the initial structure of the Wigner function remains intact, as shown in the upper graphics of Fig. 5. The oscillatory term corresponding to the off-diagonal elements of the density matrix is responsible for the coherence of the state, since the **k** distributions of the other two components (in k_y and k_z) remain unchanged. We present a direct observation of the loss of coherence in the free evolution of an entangled state. The physical model of the process of einselection is associated with annihilation of particles with different sign, initialized at regions with positive and negative values of the initial Wigner function. The Boltzmann component strives to modify the shape of the solution, until obtaining the classical equilibrium distribution, giving rise to decoherence. Scattering redistributes the momentum bringing positive and negative particles together, which causes their annihilation. The fine structure in the oscillatory term, which is the source of negative weights, is especially sensitive to this process. This term is most affected by scattering as seen in Fig. 5, in the bottom graphics. Indeed, the shape of the initial momentum distribution,

$$f(k_x) = \int dx dk_y dk_z f_w \tag{17}$$

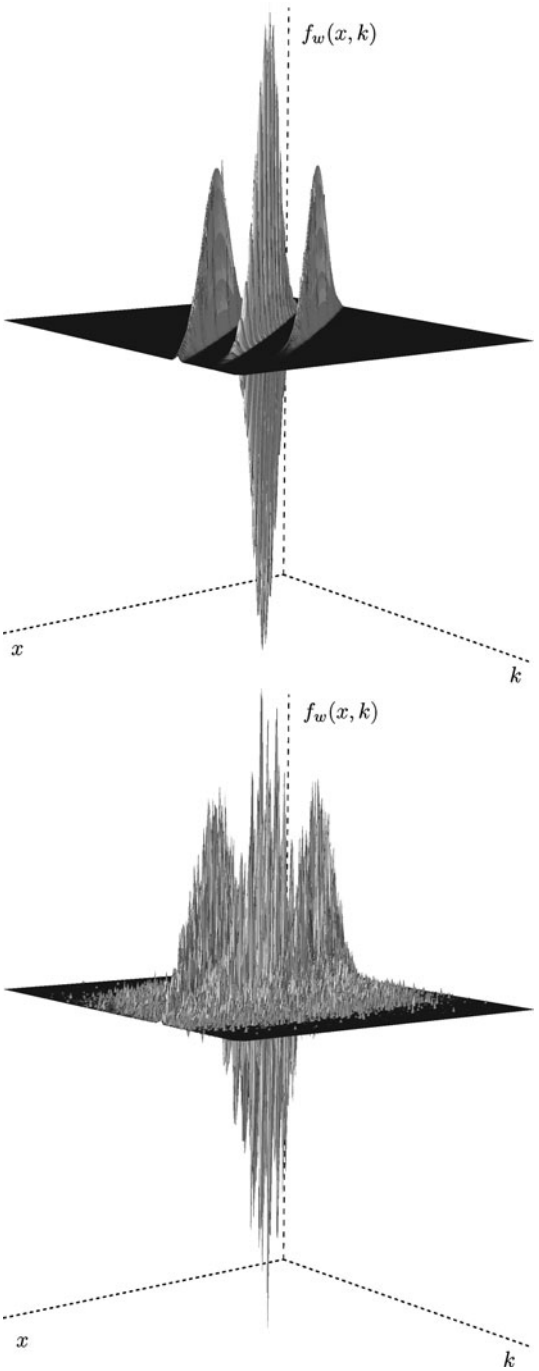

Fig. 5 *Top*: The coherent evolution leaves the basic structure of the entangled wave packets in tact even after 900 fs. *Bottom*: Scattering mechanisms destroy the initial structure of the Wigner-function as shown here after 300 fs

in Fig. 6 is due entirely to the oscillatory term, as the other two components of **k** are distributed according to thermal equilibrium, which is indicated by the thin line. The initial shape remains frozen during coherent evolution, while as is deducible from the figure, scattering destroys the coherence in about 1 ps and forces the distribution to equilibrium.

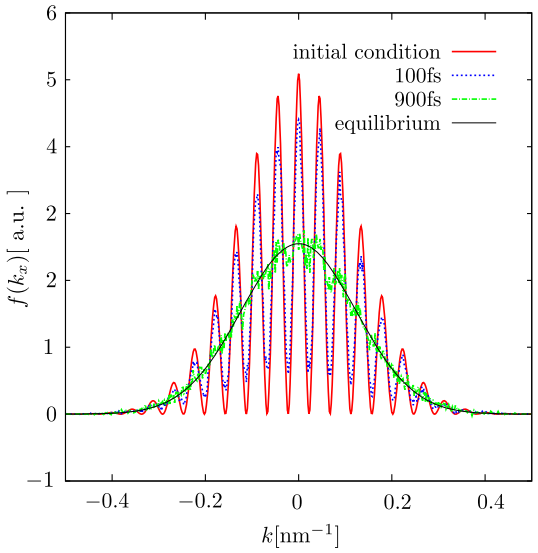

Fig. 6 The momentum distribution of the initial condition decays to the thermal equilibrium at a temperature $T = 200$ K in approximately 1 ps. Without scattering the initial distribution remains frozen in place

Figure 7 shows the density

$$n(x) = \int dk_x dk_y dk_z f_w. \tag{18}$$

The coherent curve (upper graphics) exhibits pronounced oscillations, which are suppressed in the Boltzmann curve which localizes around the initial peaks.

The initially well balanced positive and negative contributions of f_w to the density are destroyed by scattering, as seen on the bottom graphics of Fig. 7. Another effect is that scattering reduces the spreading of the wave packets as can be seen in Fig. 8. These results show that scattering induces a spatial localization and destroys coherence, thus preventing reversibility in time. Indeed the coherent wave packet is slightly broader after 200 fs, upper graphics; with this trend continuing so that the coherent wave packet begins to reach beyond the simulation domain after 500 fs, bottom graphics, while the wave packet experiencing scattering still exists completely within the confines of the simulation.

Again the retardation of the evolution is due to the randomizing effect of scattering due to phonons, which is stronger for higher energy, thus faster, particles. The interactions with phonons thus act as a kind of low pass filter with regard to the momenta within the wave packet; dampening especially the high "frequencies" and thus leading to slower propagation of the overall packet.

A measure for this behaviour is the purity P, equation (13). For coherent evolution it remains 1, while the loss

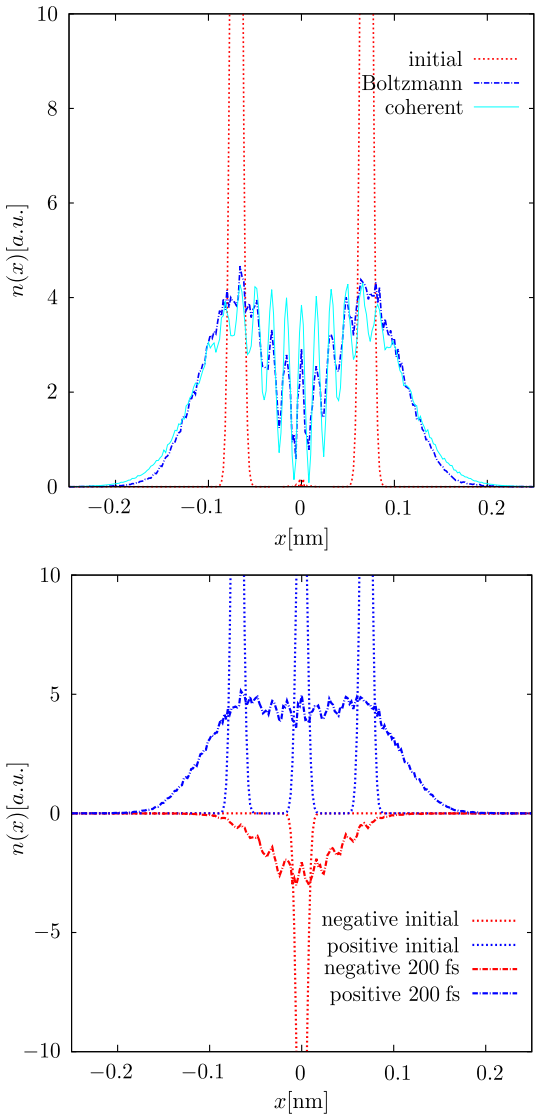

Fig. 7 *Top*: Initial, coherent and Boltzmann evolution after 200 fs at 200 K. *Bottom*: Positive and negative contributions to the density

of information in the initial state is given by its decrease. An increase of the temperature leads to an increase of the electron-phonon coupling and thus an accelerated drop of purity, as depicted in Fig. 9.

The model explains the loss of coherence with the redistribution of the negative particles. Their effect is suppressed in the sea of positive particles which dominate in the state. The pointer states which survive the monitoring by phonons are the two Gaussian packets. The initially pure state evolved towards an object having a completely different physical meaning: it is a mixed state—determined by the probabilities of the electron to be in one or the other packets related to the two wave functions.

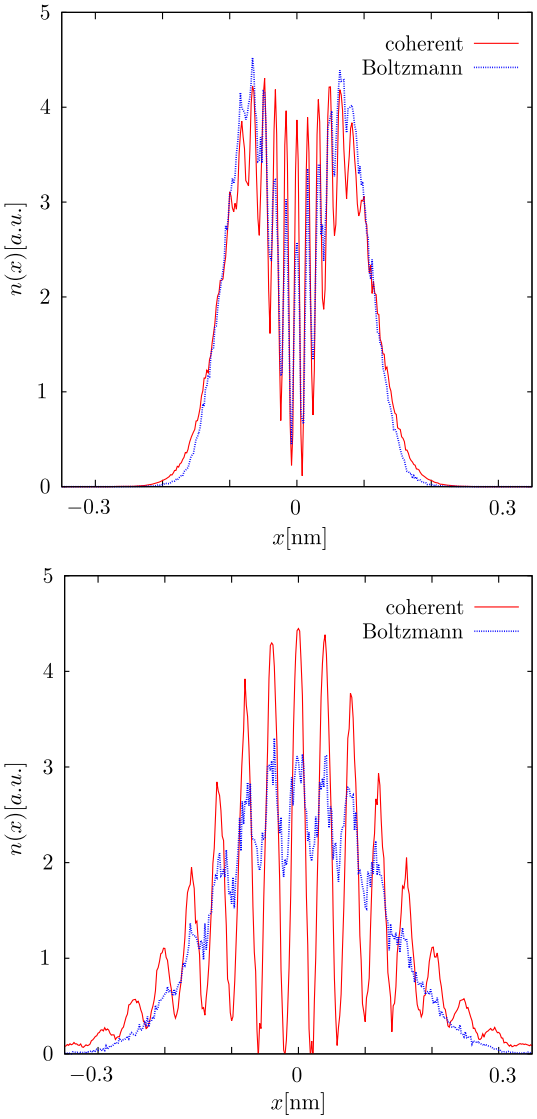

Fig. 8 The spatial broadening of the wave packet is hindered by scattering processes

4 Conclusions

The decoherence effects have been studied in two very different quantum situations: (i) a single electron wave packet interacting with a tunneling barrier; (ii) the entanglement of two wave packets. In both cases, the transition from quantum to semi-classical states is induced by electron-phonon scattering. Phonons introduced redistribute the wave vectors of the coherent physical states striving to impose the classical equilibrium distribution. The phonons introduce a time arrow in the evolution by breaking the reversibility of the coherent processes and cause localization. This analysis has been implemented by using the Wigner function formalism which offers particular advantages as: (i) a seamless transition between quantum and classical descriptions; (ii) a direct

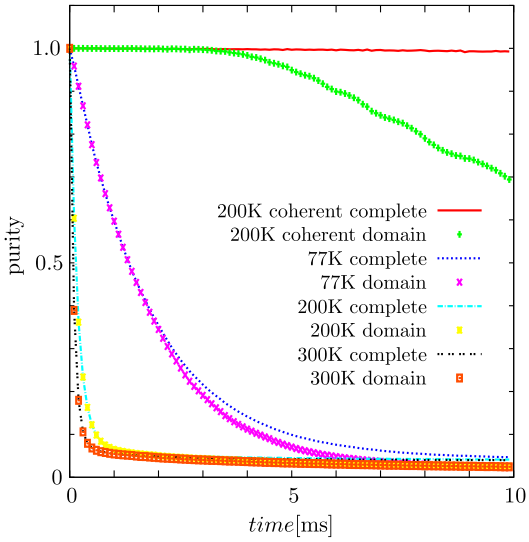

Fig. 9 Evolution of purity at different temperatures. Pairs of lines are obtained by neglecting particles which leave the simulation domain (domain) and by a complete record of all particles (complete). The former case may lead to an artificial indication for loss of coherence

inclusion of the scattering processes; (iii) ability to describe general transport regimes posed by initial and boundary conditions; and (iv) numerical feasibility to describe transient processes.

Acknowledgements This work has been supported by the Austrian Science Fund Project FWF-P21685.

References

1. Zurek, W.H.: Rev. Mod. Phys. **75**(3), 715 (2003)
2. Vacchini, B., Hornberger, K.: Relaxation dynamics of a quantum Brownian particle in an ideal gas. Eur. Phys. J. Spec. Top. **151**, 59–72 (2007)
3. Halliwell, J.J.: Two derivations of the master equation of quantum Brownian motion. J. Phys. A, Math. Theor. **40**, 3067–3080 (2007)
4. Hofheinz, M., Wang, H., Ansmann, M., Bialczak, R.C., Lucero, E., Neeley, M., O'Connell, A.D., Sank, D., Wenner, J., Martinis, J.M., Cleland, A.N.: Synthesizing arbitrary quantum states in a superconducting resonator. Nature **459**, 546–549 (2009)
5. Ferry, D.K., Akis, R., Bird, J.P.: Einselection in action: decoherence and pointer states in open quantum dots. Phys. Rev. Lett. **93**, 026803 (2004)
6. Knezevic, I.: Decoherence due to contacts in ballistic nanostructures. Phys. Rev. B **77**, 125301 (2008)
7. Joos, E., Zeh, H.D., Kiefer, C., Giulini, D.J.W., Kupsch, J., Stamatescu, I.O.: Decoherence and the Appearance of a Classical World in Quantum Theory. Springer, Berlin (2003)
8. Pastawski, H.M., Foa Torres, L.E.F., Medina, E.: Electron-phonon interaction and electronic decoherence in molecular conductors. Chem. Phys. **281**, 257–278 (2002)
9. Buscemi, F., Cancellieri, E., Bordone, P., Bertoni, A., Jacoboni, C.: Electron decoherence in a semiconductor due to electron-phonon scattering. Physica Status Solidi (c) **5**, 52–55 (2008)
10. Querlioz, D., Dollfus, P.: The Wigner Monte Carlo Method for Nanoelectronic Devices—A Particle Description of Quantum Transport and Decoherence. ISTE-Wiley, New York (2010)

11. Nedjalkov, M., Selberherr, S., Ferry, D.K., Vasileska, D., Dollfus, P., Querlioz, D., Dimov, I., Schwaha, P.: Physical scales in the Wigner-Boltzmann equation. Ann. Phys. **328**, 220–237 (2012)
12. Jacoboni, C., Brunetti, R., Bordone, P., Bertoni, A.: Quantum transport and its simulation with the Wigner-function approach. Int. J. High Speed Electron. Syst. **11**, 387–423 (2001)
13. Nedjalkov, M., Querlioz, D., Dollfus, P., Kosina, H.: Wigner function approach. In: Vasileska, D., Goodnick, S. (eds.) Nano-Electronic Devices: Semiclassical and Quantum Transport Modeling, pp. 289–358. Springer, New York (2011)
14. Shifren, L., Ringhofer, C., Ferry, D.K.: A Wigner function-based quantum ensemble Monte Carlo study of a resonant tunneling diode. IEEE Trans. Electron Devices **50**, 769–773 (2003)
15. Querlioz, D., Saint-Martin, J., Nam Do, V., Bournel, A., Dollfus, P.: A study of quantum transport in end-of-roadmap DG-MOSFETs using a fully self-consistent Wigner Monte Carlo approach. IEEE Trans. Nanotechnol. **5**, 737–744 (2006)
16. Querlioz, D., Nha Nguyen, H., Saint-Martin, J., Bournel, A., Galdin- Retailleau, S., Dollfus, P.: Wigner-Boltzmann Monte Carlo approach to nanodevice simulation: from quantum to semi-classical transport. J. Comput. Electron. **8**, 324–335 (2009)
17. Nedjalkov, M., Kosina, H., Selberherr, S., Ringhofer, C., Ferry, D.K.: Unified particle approach to Wigner-Boltzmann transport in small semiconductor devices. Phys. Rev. B **70**, 115319 (2004)
18. Sverdlov, V., Grasser, T., Kosina, H., Selberherr, S.: Scattering and spacecharge effects in Wigner Monte Carlo simulations of single and double barrier devices. J. Comput. Electron. **5**, 447–450 (2006)
19. Manfredi, G., Feix, M.R.: Entropy and Wigner functions. Phys. Rev. E **62**, 4665–4674 (2000)